I R A M P
5(2), July-Dec. 2014, pp. 123-129

ISSN: 2229-3159

Stark Broadening of Hydrogen Spectral Lines in Strongly Coupled Plasmas: Effect of the Electrostatic Plasma Turbulence at the Thermal Level

E. OKS

Physics Department, 206 Allison Lab., Auburn University, Auburn, AL 36849, USA

ABSTRACT: In 2014, Kielkopf and Allard (KA) performed a benchmark experiment where they measured the Full Width at Half Maximum (FWHM) of the H_α line at the electron densities N_e by two orders of magnitude greater than the corresponding previous benchmark experiments, namely up to $N_e = 1.4 \times 10^{20}$ cm^{-3}. No theoretical calculations of the FWHM of the H_α line existed in this range of N_e. In the present paper we present an analytical theory adequate for the range of the electron densities reached in KA experiment. In this range of N_e, a new factor becomes significant: a rising contribution of the Electrostatic Plasma Turbulence (EPT) at the *thermal* level of its energy density. After taking into account this contribution, which turns out to be comparable to the corresponding contribution by electron and ion microfields in this range of N_e, our theoretical FWHM of the H_α line becomes in a very good agreement with the experimental FWHM of the H_α line by KA in the entire range of their electron densities. We also extrapolate the FWHM of the H_α line from the Gigosos-Cardenoso tables, which were produced by the most advanced simulations, but without allowing for the thermal EPT: this leads to the underestimation of the experimental FWHM by up to 25%. Stark profiles and the FWHM of other hydrogen spectral lines can also be calculated by the present theory.

PACS numbers: 32.70.Jz, 32, 60.+i, 52.35.Fp, 52.70.Kz

1. INTRODUCTION

Benchmark experiments (i.e., experiments where plasma parameters were measured independently of the Stark broadening) played a very important role in experimental and theoretical studies of the Stark Broadening of Hydrogen Spectral Lines (SBHSL) in plasmas. As a new benchmark experiment was performed at some novel plasma source at the range of the electron densities N_e higher than for the previous benchmark experiment performed at a different plasma source, often discrepancies were found with existing theories. So, benchmark experiments stimulated developing more advanced theories – the theories allowing for various high-density effects. There is a very large amount of literature on this subject. Here we refer only to books [1, 2] and a review [3] published in the last 10 years, and references in these publications.

The most recent benchmark experiment by Kielkopf and Allard (hereafter, KA) [4], where the SBHSL was tested using the H_α line, was performed in a laser-produced pure-hydrogen plasma reaching $N_e = 1.4\times10^{20}$ cm^{-3}. This exceeded by two orders of magnitude the highest values of $N_e \sim (3 - 4)\times10^{18}$ cm^{-3} reached by the corresponding previous benchmark experiments: by Kunze group (Büscher et al [5]) at the gas-liner pinch[*/] and by Vitel group (Flih et al [6]) at the flash tube plasma.

* In the earlier experiment at the gas-liner pinch (Böddeker et al [7]), the densities up to $N_e \sim 10^{19}$ cm^{-3} had been reached. However, the experiment by Böddeker et al [7] had deficiencies, which were addressed and eliminated in the experiment by Büscher et al [5]. In distinction to the former experiment, in the latter one: a) the spectroscopic measurements were performed simultaneously with the diagnostics; b) highly reproducible discharge condition was used where the H_α line was measured spatially resolved along the discharge axis indicating that no inhomogeneities along the axis existed; c) high care has been taken to prevent the optical thickness.

No theoretical calculations of the Full Width at Half Maximum (FWHM) of the H_α line existed at the electron densities reached in KA experiment [4]. Indeed, the highest value of N_e in the tables of FWHM of the H_α line by Gigosos and Cardenoso [8], produced by fully-numerical simulations, was 4.64×10^{18} cm^{-3}(their simulations are considered by the research community as the most advanced). In frames so-called standard (or conventional) analytical theory, Kepple and Griem [9] calculated the FWHM of the H_α line up to $N_e = 10^{19}$ cm^{-3}, because at higher values of N_e the standard theory becomes invalid. (The primary distinction between the standard analytical theory [9] and Gigosos-Cardenoso simulations [8] is that the latter allowed for the ion dynamics in distinction to the former; however, the role of the ion dynamics diminishes as N_e increases and becomes practically insignificant at values of $N_e \sim 10^{19}$ cm^{-3} and higher.) All other simulations and analytical methods, reviews of which can be found, e.g., in book [1] and paper [3], listed the FWHM of the H_α line either up to $N_e \sim 4\times10^{18}$ cm^{-3} or lower.

Therefore, in the present paper we develop an analytical theory that is adequate for the range of the electron densities reached in KA experiment [4]. At this range of N_e, a new factor becomes significant for the SBHSL – the factor never taken into account in any previous simulations or analytical theories of the SBHSL. This new factor is a rising contribution of the Electrostatic Plasma Turbulence (EPT) at the *thermal* level of its energy density.

The EPT at any level of its energy density is represented by oscillatory electric fields F_t arising when the waves of the separation of charges propagate through plasmas: they correspond to *collective degrees of freedom* in plasmas – in distinction to the electron and ion microfields that correspond to individual degrees of freedom of charged particles. In relatively low density plasmas, various kinds of the EPT at the *supra-thermal* levels of its energy density, specifically at the levels several orders of magnitude higher than the thermal level, were discovered experimentally via the enhanced ("anomalous") SBHSL in numerous experiments performed by different groups at various plasma sources [10-23], some of these experiments being summarized in book [24].

As for the EPT at the thermal level of its energy density (hereafter, "thermal EPT"), their contribution to the SBHSL in relatively low density plasmas is by several orders of magnitude smaller than the contribution of the electron and ion microfields, so that their effect was negligibly small and therefore never detected spectroscopically. However, at the range of the electron densities reached in KA experiment [4], the contribution to the SBHSL from the thermal EPT becomes comparable to the contribution of the electron and ion microfields.

In the present paper we take into account the contribution to the SBHSL from the thermal EPT. As a result, the theoretical FWHM of the H_α line becomes in a very good agreement with the experimental FWHM of the H_α line by KA [4] in the entire range of their electron densities, including the highest electron density $N_e = 1.4\times10^{20}$ cm^{-3}. We also show that the extrapolation of the FWHM of the H_α line from the Gigosos-Cardenoso tables [8], which were produced by the most advanced simulations, leads to the underestimation of the experimental FWHM at $N_e = 1.4\times10^{20}$ cm^{-3} by 25%.

2. THEORY AND THE COMPARISON WITH THE EXPERIMENT

According to Bohm and Pines [25[, the number of collective degrees of freedom in a unit volume of a plasma is $N_{coll} = 1/(6\pi^2 r_D^3)$, where r_D is the Debye radius. Therefore the energy density of the oscillatory electric fields at the thermal level is $F_t^2/(8\pi) = N_{coll}T/2$, so that

$$F_t^2 = 16\pi^{1/2}e^3N_e^{3/2}/(3T^{1/2}), \tag{1}$$

where T is the temperature and e is the electron charge.

At the absence of a magnetic field, there are only two types of the EPT: Langmuir waves/turbulence and ion acoustic waves/turbulence (a.k.a. ionic sound). Langmuir waves are the high-frequency branch of the EPT. Its frequency is approximately the plasma electron frequency

$$\omega_{pe} = (4\pi e^2N_e/m_e)^{1/2} = 5.64\times10^4\ N_e^{1/2} \tag{2}$$

Ion acoustic waves are the low-frequency branch of the EPT. They are represented by a broadband oscillatory electric field, whose frequency spectrum is below or of the order of the ion plasma frequency

$$\omega_{pi} = (4\pi e^2 N_i Z^2/m_i)^{1/2} = 1.32\times10^3\ Z(N_i m_p/m_i)^{1/2}, \tag{3}$$

where N_i is the ion density, Z is the charge state; m_e, m_p, and m_i are the electron, proton and ion masses, respectively. In the "practical" parts of Eqs. (2) and (3), CGS units are used. Below we set Z = 1, so that $N_i = N_e$.

The thermal energy density of the collective degrees of freedom $F_t^2/(8\pi) = N_{coll}T/2$ is distributed in equal parts between the high- and low-frequency branches:

$$F_0^2 = E_0^2 = F_t^2/2, \tag{4}$$

where F_0 and E_0 are the root-mean-square (rms) thermal electric fields of the ion acoustic turbulence and the Langmuir turbulence, respectively.

Let us first discuss the contribution of the thermal ion acoustic turbulence to the SBHSL. It is useful to begin by estimating a ratio of the rms thermal electric field F_0 of the ion acoustic turbulence to the standard characteristic value F_N of the ion microfield, where

$$F_N = 2\pi(4/15)^{2/3} e N_e^{2/3} = 2.603\ e N_e^{2/3} = 3.751\times10^{-7}\ [N_e(\mathrm{cm}^{-3})]^{2/3}\ \mathrm{V/cm} \tag{5}$$

Using Eqs. (1), (4), (5), we obtain:

$$F_0/F_N = 0.1689\ N_e^{1/12}/[T(K)]^{1/4}, \tag{6}$$

where the temperature T is in Kelvin. At the highest density point of KA experiment [4] ($N_e = 1.39\times10^{20}$ cm^{-3}, T = 34486 K), Eq. (6) yields $F_0/F_N = 0.59$. This shows that in the conditions of KA experiment [4], the rms thermal electric field of the ion acoustic turbulence becomes comparable to the standard ion microfield.

In a broad range of plasma parameters, especially at the range of densities of KA experiment [4], radiating hydrogen atoms perceive oscillatory electric fields of the ion acoustic turbulence as quasistatic. In any code designed for calculating shapes of spectral lines from plasmas, an important task becomes the averaging over the ensemble distribution W(**F**) of the *total* quasistatic field $\mathbf{F} = \mathbf{F}_t + \mathbf{F}_i$, where $\mathbf{F}_i$ is the quasistatic part of the ion microfiled (for the range of densities of KA [4] almost the entire ion microfiled is quasistatic). In other words, the key part of the problem becomes the calculation of W(**F**).

The distribution of a low-frequency turbulent field was derived in paper [26]. In the isotropic case it can be represented in the following form

$$W_t(a, x)dx = 3[6/\pi]^{1/2} a^3 x^2 \exp(-3a^2 x^2/2)]dx, \tag{7}$$

where

$$x = F_t/F_N,\ a = F_0/F_N. \tag{8}$$

The total quasistatic field **F** results from the vector summation of the two statistically independent contributions: $\mathbf{F} = \mathbf{F}_t + \mathbf{F}_i$. The justification of this has been given in papers by Ecker and Fisher [27] and Spatscheck [28]. Therefore the distribution $W(F/F_N)$ of the total field is a convolution of the distribution $W_t(F_t/F_N)$ of the turbulent field with the distribution $W_i(F_i/F_N)$ of the ion microfield:

$$W(\beta)d\beta = [\ \iint d\mathbf{x}d\mathbf{u}\ W_i(\mathbf{u})W_t(\mathbf{x})\delta(\beta - \beta_s)]d\beta,\ \beta = F/F_N,\ \mathbf{x} = \mathbf{F}_i/F_N,\ \mathbf{u} = \mathbf{F}_i/F_N. \tag{9}$$

Here

$$\beta_s = |\mathbf{x} + \mathbf{u}| = (x^2 + u^2 - 2ux\cos\theta)^{1/2}, \tag{10}$$

where θ is the angle between vectors **u** and **x**. Using the properties of the δ-function, Eq. (9) has been simplified in paper [26] as follows:

$$W(a, \beta) = [3/(2\pi)^{1/2}]\, a\beta \int du\{\exp[-3a^2(\beta - u)^2] - \exp[-3a^2(\beta + u)^2]\}W_i(u)/u. \tag{11}$$

For the distribution of the quasistatic part of the ion microfield $W_i(u)$ in Eq. (12) we use here the APEX distribution [29].

Now let us discuss the contribution of the thermal Langmuir turbulence to the SBHSL. The Langmuir turbulence, being the high-frequency one, causes a *dynamical* SBHSL – similar to the dynamical SBHSL by the electron microfield. In paper [30] there was derived analytically the Langmuir-turbulence-caused contribution (additional to the electron microfield contribution) to the real part $\Gamma = -\,\mathrm{Re}\,\Phi$ of the dynamical broadening operator Φ. In particular, diagonal elements of Γ have the form

$$\Gamma_{\alpha\beta} = \Gamma_\alpha + \Gamma_\beta - d_{\alpha\alpha}\, d_{\beta\beta}\, E_0{}^2\gamma_p/[3\hbar^2(\gamma_p{}^2 + \omega_{pe}{}^2)], \tag{12}$$

where

$$\Gamma_\alpha=[E_0{}^2\gamma_p/(12\hbar^2)]\{2\mathbf{d}_{\alpha\alpha}{}^2/(\gamma_p{}^2+\omega_{pe}{}^2) +(|\,\mathbf{d}_{\alpha,\,\alpha-1}|^2+|\,\mathbf{d}_{\alpha,\,\alpha+1}|^2)[1/(\gamma_p{}^2+(\omega_F-\omega_{pe})^2) + 1/(\gamma_p{}^2+(\omega_F+\omega_{pe})^2)]\}, \tag{13}$$

The formula for Γ_β entering Eq. (12) can be obtained from Eqs. (13) by substituting the subscript α by β. Here α and β label Stark sublevels of the upper (a) and lower (b) levels involved in the radiative transition, respectively; $\omega_F = 3n_\alpha\hbar F/(2m_e e)$ is the separation between the Stark sublevels caused by the total quasistatic electric field F; the matrix elements of the dipole moment operator are

$$\mathbf{d}_{\alpha\alpha}{}^2 =[3ea_0n_\alpha q_\alpha/(2)]^2,\ |\,\mathbf{d}_{\alpha,\,\alpha-1}|^2-|\,\mathbf{d}_{\alpha,\,\alpha+1}|^2 =\mathbf{d}_{\alpha\alpha}{}^2/q_\alpha,\ |\,\mathbf{d}_{\alpha,\,\alpha-1}|^2+|\,\mathbf{d}_{\alpha,\,\alpha+1}|^2) =\mathbf{d}_{\alpha\alpha}{}^2(n^2\text{-}q^2\text{-}m^2\text{-}1)_\alpha/(2q_\alpha{}^2), \tag{14}$$

where a_0 is the Bohr radius, n is the principal quantum number, $q = n_1 - n_2$ is the electric quantum number; n_1, n_2 and m are the parabolic quantum numbers. In Eq. (14) in the subscripts we used the notation $\alpha+1$ and $\alpha-1$ for the Stark sublevels of the energies $+\hbar\omega_F$ and $-\hbar\omega_F$, respectively (compared to the energy of the sublevel α).

The quantity γ_p in Eqs. (12), (13) is the sum of the characteristic frequencies of the following processes in plasmas: the electron-ion collision rate γ_{ei} and the average Landau damping rate γ_L (see, e, g, [31]), as well as the characteristic frequency γ_{ind} of the nonlinear mechanism of the induced scattering of Langmuir plasmons on ions (see, e.g., [32]):

$$\gamma_p = \gamma_{ei} + \gamma_L + \gamma_{ind}. \tag{15}$$

The frequency γ_p controls the width of the power spectrum of the Langmuir turbulence.

At the highest density point of KA experiment [4] ($N_e = 1.39\times10^{20}$ cm^{-3}, T = 34486 K), the ratio of the thermal-Langmuir-turbulence-caused contribution to the dynamical Stark width of the H_α line to the corresponding contribution by the ion microfield reaches the value ~ 0.1.

We calculated Stark profiles of the H_α line with the allowance for the above two effects of the thermal EPT. We used the formalism of the core generalized theory of the SBHSL [33, 1] modified according to [34] to allow for incomplete collisions†.

The core generalized theory is based on using atomic states dressed by a *broad-band* field of plasma electrons and ions. These generalized dressed atomic states is a more complicated concept than the usual dressed atomic states, where the dressing was due to a monochromatic field (such as, e.g., a laser field).

† While some later additions to the generalized theory, such as, e.g., the effect of the acceleration of perturbing electrons by the ion field, caused a difference of opinions in the literature, in the rigorous analytical results of the core generalized theory there was never found any flaw.

The employment of the generalized dressed atomic allowed to describe analytically a coupling of the electron and ion microfields facilitated by the radiating atom. The coupling increases with the principal quantum number n and with the electron density N_e. Besides, it increases as the temperature T decreases.

In the present paper we modified the formalism of the generalized theory from [34] to allow for the thermal EPT. Namely, we used the distribution of the total quasistatic microfield given by Eq. (11), thus allowing for the low-frequency thermal EPT, and also added the contribution of the high-frequency thermal EPT to the dynamical broadening operator Φ.

Figure 1 shows the comparison of the FWHM of the H_α line from KA experiment [4] (dots) with the corresponding FWHM yielded by our present analytical theory (solid line). It is seen that the agreement is very good. Even at the highest density point of KA experiment [4] ($N_e = 1.39\times10^{20}$ cm^{-3}, T = 34486 K), our theoretical FWHM differs by just 4.5% from the most probable experimental value and is well within the experimental error margin.

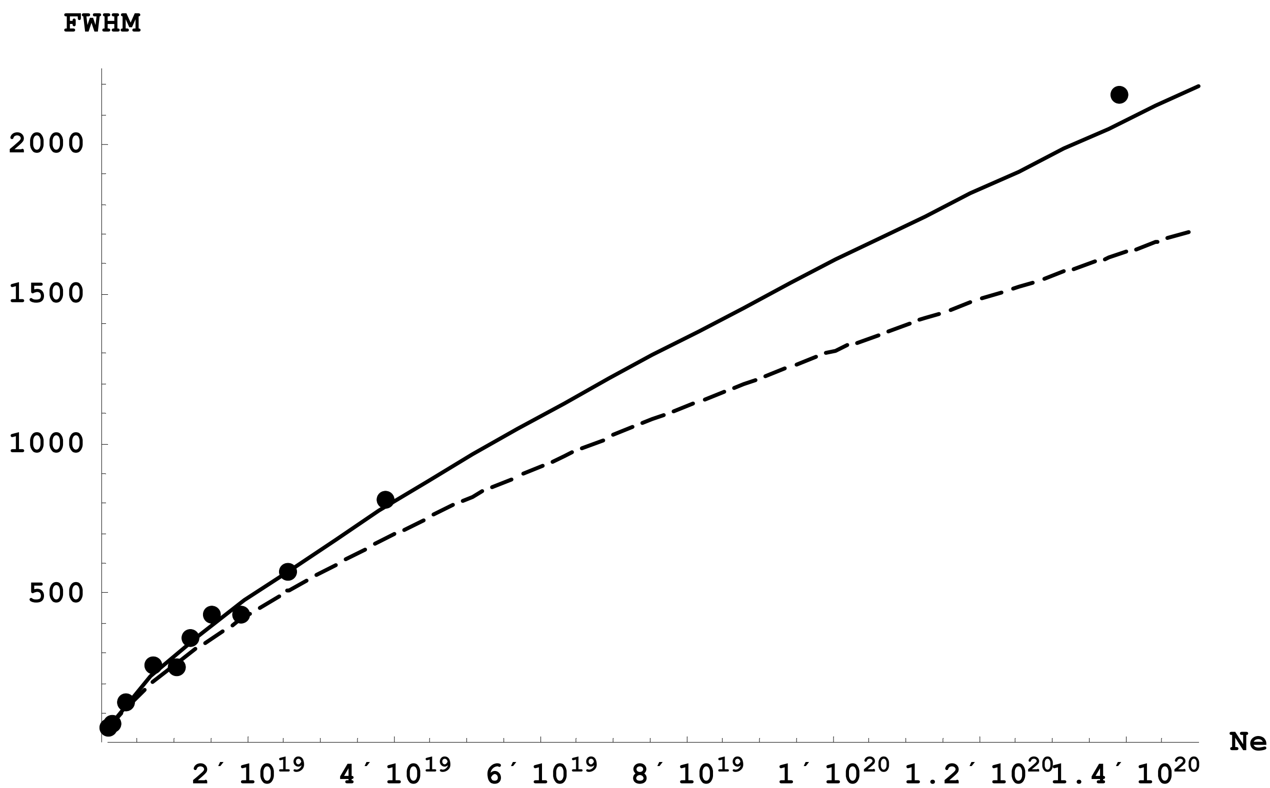

Fig. 1. Comparison of the FWHM of the H_α line from Kielkopf-Allard experiment [4] (dots) with the corresponding FWHM yielded by our present analytical theory (solid line) and by Gigosos-Cardenoso simulations [8] (dashed line).

Figure 1 shows also the FWHM obtained by extrapolating the corresponding theoretical data from Gigosos-Cardenoso tables [8] (dashed line). It is seen that Gigosos-Cardenoso FWHM is significantly below the corresponding experimental FWHM at the electron densities higher than 2×10^{19} cm^{-3}. In particular, at the highest density point of KA experiment [4] ($N_e = 1.39\times10^{20}$ cm^{-3}, T = 34486 K), Gigosos-Cardenoso FWHM underestimates the experimental FWHM by 25%, which is beyond the experimental error margin almost by a factor of two. This is no wonder: while their simulations were the most advanced (at the absence of the EPT), they did not take into account the effects of the thermal EPT, which become more and more important as the plasma becomes more strongly coupled.

3. CONCLUSIONS

We took into account the contribution to the Stark broadening from the *thermal* electrostatic plasma turbulence. We showed that this contribution becomes comparable to the corresponding contribution by electron and ion microfields at this range of electron density.

As a result, the theoretical FWHM of the H_α line became in a very good agreement with the experimental FWHM of the H_α line by Kielkopf-Allard [4] in the entire range of their electron densities, including the highest electron density $N_e = 1.4\times10^{20}$ cm^{-3}. We also showed that the extrapolation of the FWHM of the H_α line from the Gigosos-Cardenoso tables [8], which were produced by the most advanced simulations, but without allowing for the thermal electrostatic plasma turbulence, led to the underestimation of the experimental FWHM by up to 25%.

The present theory can be also used for calculating Stark profiles and the FWHM of other hydrogen spectral lines.

References

[1] Oks E 2006 *Stark Broadening of Hydrogen and Hydrogenlike Spectral Lines in Plasmas: The Physical Insight* (Oxford: Alpha Science International)

[2] Kunze H J 2009 *Introduction to Plasma Spectroscopy* (Berlin: Springer)

[3] Gigosos M A 2014 *J. Phys. D: Appl. Phys.* **47** *343001*

[4] Kielkopf J F and Allard N F 2014 *J. Phys. B: At. Mol. Opt. Phys.***47** 155701

[5] Büscher S, Wrubel T, Ferri S and Kunze H J 2002 *J. Phys. B: At. Mol. Opt. Phys.***35** 2889

[6] Flih S A, Oks E and Vitel Y 2003 *J. Phys. B: At. Mol. Opt. Phys.* **36** 283

[7] Böddeker St, Günter S, Könies A, Hitzschke L and Kunze H J 1993 *Phys. Rev.*E **47** 2785

[8] Gigosos M A and Cardenoso V 1996 2003 *J. Phys. B: At. Mol. Opt. Phys.* **29** 4795

[9] Kepple P and Griem H R 1968 *Phys. Rev.* **173** 317

[10] Antonov A S, Zinov'ev O A, Rusanov V D and Titov A V 1970 *Zh. Exper. Teor. Fiz.* (*Sov. Phys. JETP*) **58** 1567

[11] Zagorodnikov S P, Smolkin G E, Striganova E A and Sholin G V 1970 *Pis'ma v Zh. Exper. Teor. Fiz.* (*Sov. Phys. JETP Letters*) **11** 475; 1970 *Doklady Akad. Nauk SSSR* (*Sov. Phys. Doklady*) **195** 1065

[12] Zavojskij E K, Kalinin Ju G, Skorjupin V A, Shapkin V V and Sholin G V 1970 *Doklady Akad. Nauk SSSR* (*Sov. Phys. Doklady*) **194** 55; 1970 *Pis'ma v Zh. Exper. Teor. Fiz.* (*Sov. Phys. JETP Letters*) **13** 19

[13] Levine M A and Gallagher C C 1970 *Phys. Letters* **A32** 14

[14] Ben-Yosef N and Rubin A G 1970 *Phys. Letters* **A33** 222

[15] Zakatov L P, Plakhov A G, Shapkin V V and Sholin G V1971 *Doklady Akad. Nauk SSSR* (*Sov. Phys. Doklady*) **198** 1306

[16] Berezin A B, Dubovoj A V and Ljublin B V 1971 *Zh. Tekhnich. Fiz.* (*Sov. Phys. Tech. Phys.*) **41** 2323

[17] Babykin M V, Zhuzhunashvili A I, Oks E, Shapkin V V and Sholin G V 1973 *Zh. Exper. Teor. Fiz.* (*Sov. Phys. JETP*) **65** 175

[18] Volkov Ja F, Djatlov V G and Mitina A I 1974 *Zh. Tekhnich. Fiz.* (*Sov. Phys. Tech. Phys.*) **44**, 1448

[19] Zhuzhunashvili A I and Oks E 1977 *Sov. Phys. JETP* **46**, 2142

[20] Oks E and Rantsev-Kartinov V A 1980 *Sov. Phys. JETP* **52** 50

[21] Berezin A B, Ljublin B V and Jakovlev D G 1983 *Zh. Tekhnich. Fiz.* (*Sov. Phys. Tech. Phys.*) **53**, 642

[22] Koval A N and Oks E 1983 *Bull. Crimean Astrophys. Observ.* **67** 78

[23] Oks E, Böddeker St and Kunze H J 1991 *Phys. Rev.* A **44** 8338

[24] Oks E 1995 *Plasma Spectroscopy: The Influence of Microwave and Laser Fields*, Springer Series on Atoms and Plasmas, vol. 9 (Berlin: Springer)

[25] Bohm D and Pines D 1953 *Phys. Rev.* **92** 609

[26] Oks, E., & Sholin, G.V. 1976, *Sov. Phys. Tech. Phys.,* 21, 144.

[27] Ecker G H and Fisher K G 1971 *Z. Naturforsch.* **26a** 1360

[28] Spatschek K H 1974 *Phys. Fluids* **17** 969

[29] Iglesias C A, DeWitt H E, Lebowitz J L, MacGowan D and Hubbard W B 1985 *Phys. Rev.* A **31** 1698

[30] Oks E and Sholin G V 1975 *Sov. Phys. JETP* **41** 482

[31] Bellan P M 2006 *Fundamentals of Plasma Physics* (Cambridge: Cambridge University Press)

[32] Kadomtsev B B 1988 *Collective Phenomena in Plasma* (Moscow: Nauka)

[33] Ispolatov Ya and Oks E 1994 *J. Quant. Spectrosc. Rad. Transfer* **51** 129

[34] Oks E 2006 *18th Int. Conf. "Spectral Line Shapes"* (Auburn, AL), invited paper, *AIP Conf. Proc.* **874** 19